JACS Au
AN OPEN ACCESS JOURNAL OF THE AMERICAN CHEMICAL SOCIETY

pubs.acs.org/jacsau

Article

Biodegradable Block Copolymer–Tannic Acid Glue

Jongmin Park,[⊥] Eunsook Park,[⊥] Siyoung Q. Choi, Jingxian Wu, Jihye Park, Hyeonju Lee, Hyungjun Kim, Haeshin Lee,* and Myungeun Seo*

Cite This: https://doi.org/10.1021/jacsau.2c00241

Read Online

ACCESS | Metrics & More | Article Recommendations | Supporting Information

ABSTRACT: Bioadhesives are becoming an essential and important ingredient in medical science. Despite numerous reports, developing adhesive materials that combine strong adhesion, biocompatibility, and biodegradation remains a challenging task. Here, we present a biocompatible yet biodegradable block copolymer-based waterborne superglue that leads to an application of follicle-free hair transplantation. Our design strategy bridges self-assembled, temperature-sensitive block copolymer nanostructures with tannic acid as a sticky and biodegradable polyphenolic compound. The formulation further uniquely offers step-by-step increases in adhesion strength via heating–cooling cycles. Combining the modular design with the thermal treating process enhances the mechanical properties up to 5 orders of magnitude compared to the homopolymer formulation. This study opens a new direction in bioadhesive formulation strategies utilizing block copolymer nanotechnology for systematic and synergistic control of the material's properties.

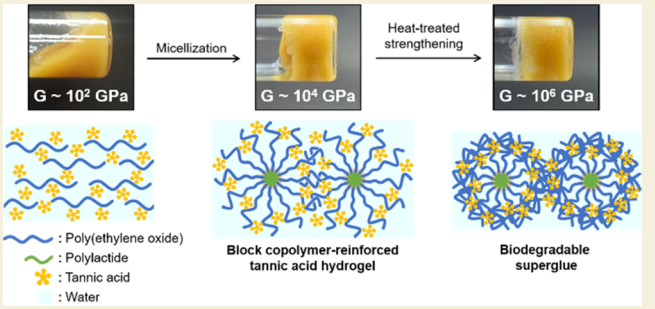

KEYWORDS: *bioadhesive, hydrogel, block polymer micelle, tannic acid, heat-treated*

Downloaded via 69.174.157.23 on September 24, 2022 at 17:29:55 (UTC).
See https://pubs.acs.org/sharingguidelines for options on how to legitimately share published articles.

INTRODUCTION

Medical adhesives are being extensively investigated for diverse applications such as wound healing, hemostasis, sealants after anastomosis, and tissue engineering.[1,2] However, considerable challenges remain in the development of medical adhesives to satisfy all of the following three criteria: (1) high adhesion, (2) biocompatibility showing a low level of acute and chronic inflammations, and (3) degradation by hydrolysis. Despite numerous studies, no bioadhesives exhibiting all three properties exist. Naturally found proteins such as fibrin and collagen are biocompatible and degraded by enzymatic reactions, but the weak tissue adhesions limit their applications in a wide range of clinical settings.[2] In contrast, highly adhesive synthetic glues based on polyurethane and polycyanoacrylate suffer from toxicity that causes inflammatory immune responses.[3]

Mussel- and plant-inspired phenolic or phenolamine glues are appealing alternatives to medical applications. They employ strong and versatile interactions provided by the phenolic moieties such as catechol and gallol (Figure 1a). Medical adhesives possessing phenolic groups conjugated onto biopolymers generally exhibit a reasonably low level of toxicity. Examples include chitosan–catechol,[4,5] chitosan–gallol, alginate–catechol,[6,7] glycol chitosan–catechol,[8] dextran–catechol,[9] and poly(ethylene glycol)–catechol.[10] These bioinspired adhesives largely vary in adhesion performance depending on the types of backbone and the phenolic motif, as well as the conjugation degree. For example, a gallol-conjugated polymer exhibited about 7 times stronger adhesion than the catechol analogue due to the tridentate cross-linking mechanism.[11] Their degradability, however, is typically low in vivo. While synthetic vinyl polymer-based glues containing catechol pendants have been also explored as functional adhesives,[12−15] low in vivo degradability of the C–C main chain would also limit their medical applications.

Another class is a blend of synthetic water-soluble polymer with polyphenols (Figure 1b).[16−22] Tannins, plant polyphenolic compounds such as tannic acid (TA), can coagulate the polymer in water into a sticky viscoelastic liquid via multiple hydrogen bonds.[23,24] We have previously reported that poly(ethylene oxide) and poly(vinyl alcohol) can form adhesives with TA.[16,21] Since TA is a hydrolyzable tannin and also edible, biocompatibility and degradability can be achieved by the choice of the polymer. However, improving adhesion properties has been challenging because of the inherently low elastic modulus.

To simultaneously address all three issues of strong adhesion, suitable biocompatibility, and controllable biode-

Received: April 18, 2022
Revised: August 11, 2022
Accepted: August 12, 2022

© XXXX The Authors. Published by American Chemical Society

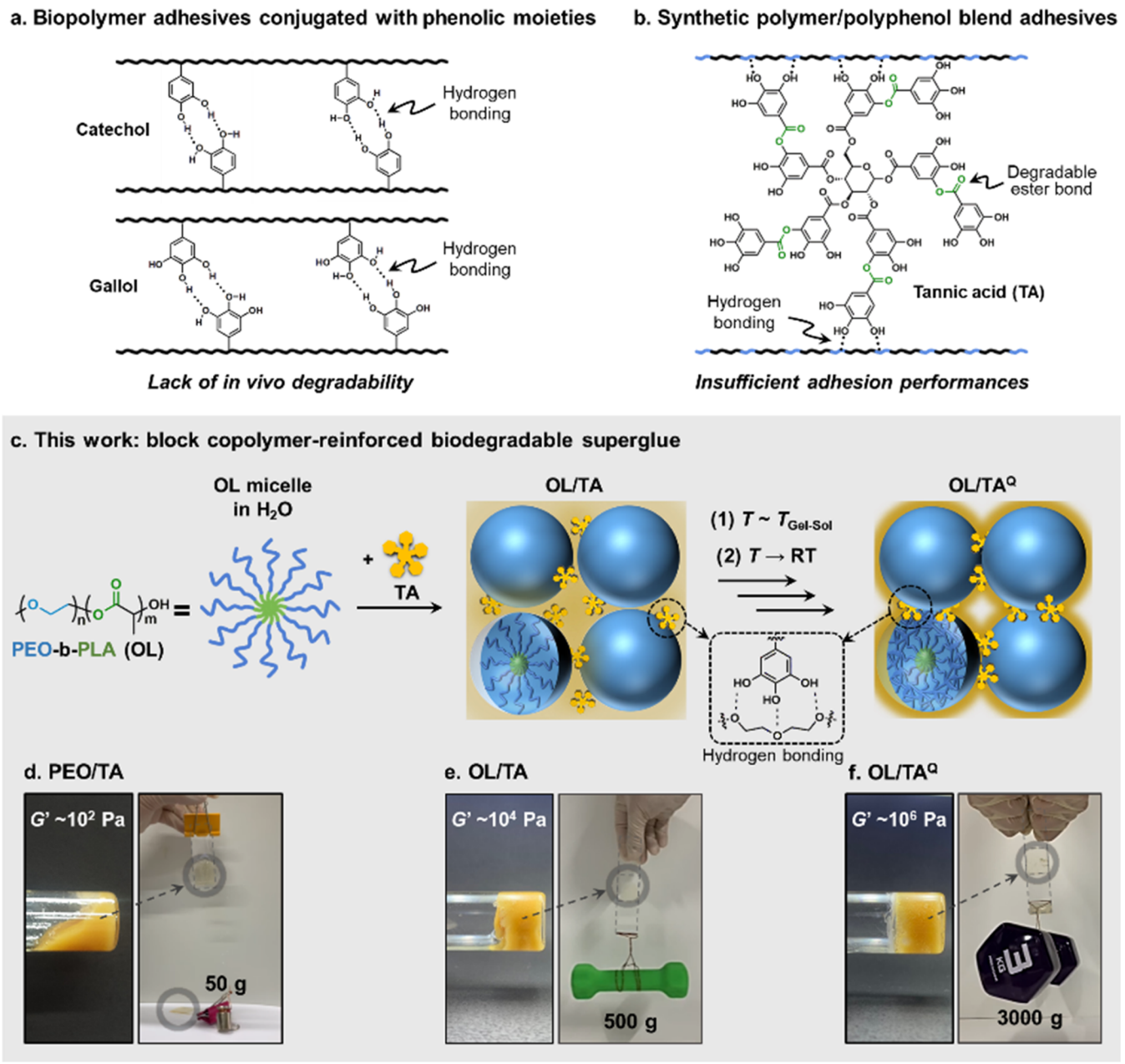

Figure 1. Block copolymer-reinforced biodegradable superglue. (a, b) Previously studied classes of bioadhesives based on phenolic moieties. (a) Catechol- and gallol-conjugated biopolymers. (b) Blend of synthetic water-soluble polymers with polyphenols. Tannic acid (TA) is given as a representative polyphenol, and the degradable ester linkage is shown in green. (c) Blend of an amphiphilic diblock copolymer with TA in this study. PEO-*b*-PLA (OL) consisting of hydrophilic and temperature-sensitive poly(ethylene oxide) (PEO) and hydrophobic poly(lactic acid) (PLA) was chosen as a biocompatible and biodegradable block copolymer. OL micelles form in water driven by hydrophobic interaction and associate with TA via hydrogen bonding of phenolic hydroxyl groups with PEO corona to produce an OL/TA gel at a high concentration. Repeatedly heating the gel close to the gel−sol transition and cooling back to room temperature strengthens the material by reorganizing the hydrogen-bonded network with the dehydration−rehydration process of the PEO corona. (d−f) Photos of OL/TA and heat-treated OL/TA^{Q} compared to the blend of TA with the PEO homopolymer (PEO/TA). G' values obtained at ω = 10 rad s^{-1} and γ = 1% are shown within the photos. Adhesion strength was demonstrated by dumbbell lifting for 15 s. (d) PEO/TA. (e) OL-M/TA, and (f) OL-M/TA^{Q}.

gradation, we designed a new adhesive formulation consisting of an amphiphilic, biodegradable, and also biocompatible block copolymer and TA (Figure 1c). The key is to use poly(ethylene oxide)−poly(lactic acid) diblock copolymer (PEO-*b*-PLA). Both PEO and PLA are widely used biocompatible polymers approved by the U.S. Food and Drug Administration (FDA), and PLA is a renowned bioplastic known particularly for its hydrolytic susceptibility.[25−27] The block copolymer self-assembles into micelles with a PLA core and a PEO corona in water to avoid unfavorable exposure to the hydrophobic PLA and has also been approved for clinical trials as a drug delivery vector.[28−30] In the presence of TA, the PEO corona containing oxygen atoms along the chain interacts with TA to produce a three-dimensional micellar network bridged by TA.[16] In contrast to the TA−homopolymer complexes, the PLA core reinforces the water-swollen network, resulting in a viscoelastic solid, a hydrogel with dramatically

https://doi.org/10.1021/jacsau.2c00241
JACS Au XXXX, XXX, XXX−XXX

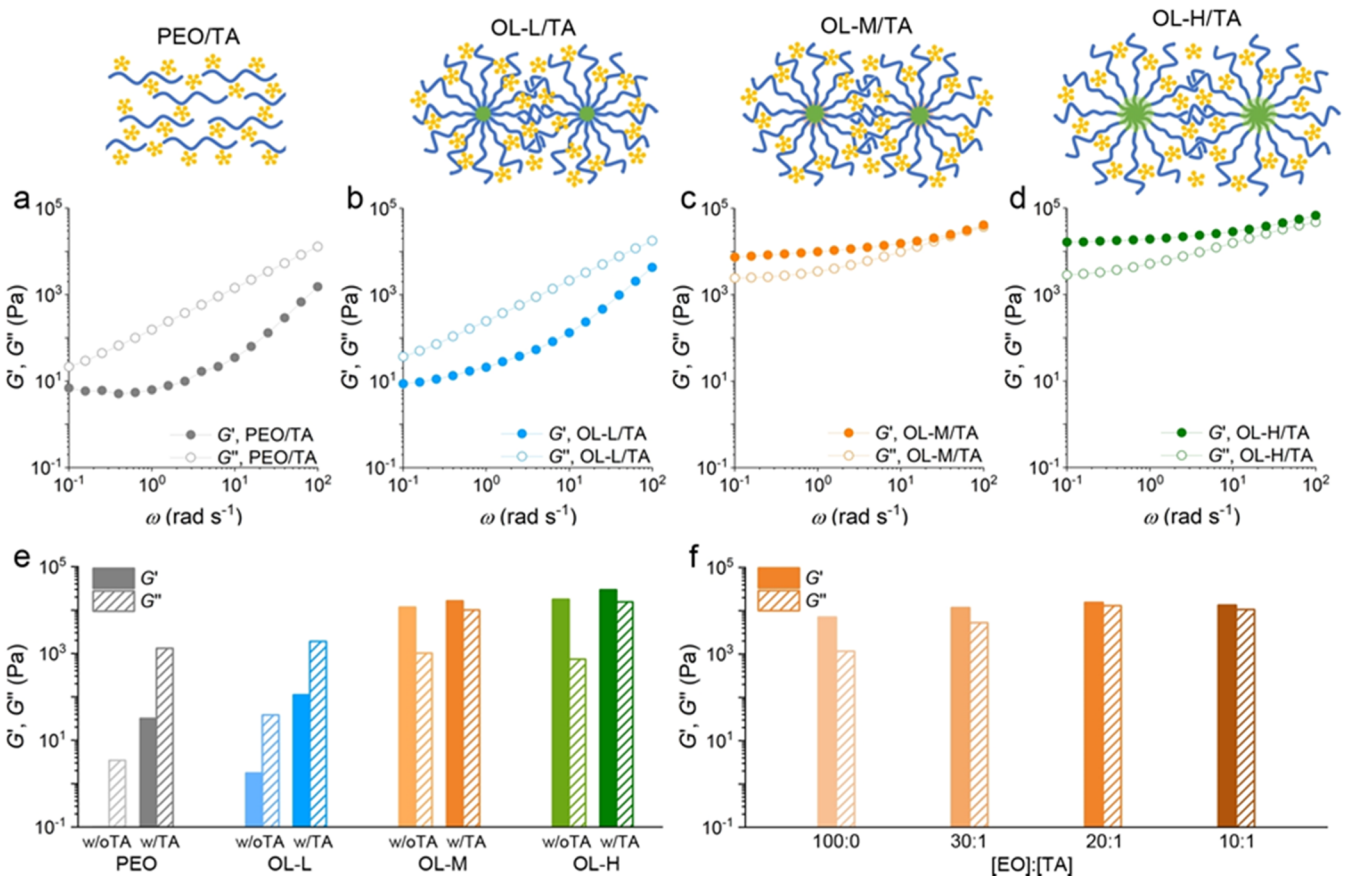

Figure 2. Mechanical enhancement in OL/TAs compared to PEO/TA. (a–d) Frequency sweep data of PEO/TA and OL/TA formed with the mixing ratio of [EO]/[TA] = 20:1. (e, f) Change in dynamic moduli as a function of f_{PLA} (e) and [EO]/[TA] in OL-M/TA (f). The moduli obtained at ω = 10 rad s^{-1} and γ = 1% are presented. In (e), the [EO]/[TA] ratio is fixed as 20:1.

increased mechanical properties. The TA–PEO interaction preserves the necessary sticky nature of an adhesive.

Herein, we demonstrate the concept of a block copolymer–TA superglue with a series of PEO-*b*-PLA. Simply mixing aqueous solutions of PEO-*b*-PLA and TA produces a sticky coacervate hydrogel with mechanical properties that can be tuned by varying the composition (Figure 1c).

Compared to the PEO/TA mixture, the elastic modulus was enhanced up to 3 orders of magnitude, producing a much tougher adhesive with higher shear strength (Figure 1d,e). More importantly, we demonstrate that applying heating cycles to the hydrogel can further increase the elastic modulus by >200-fold (Figure 1f). The temperature-dependent PEO solubility enables this unique hardening process through thermal cycles, via redistribution and densification of the hydrogen-bonded network. The improved mechanical properties are retained much longer with the block copolymer than PEO. The heat-treated block copolymer-containing hydrogels exhibited superior adhesion performance, allowing us to realize an unprecedented application of follicle-free hair transplantation.

RESULTS AND DISCUSSION

Preparation of OL/TA Glue

Three PEO-*b*-PLAs were prepared via ring-opening polymerization of D,L-lactide (LA) in the presence of methoxy-terminated PEO with a number average molar mass of 20 kg mol^{-1} (for characterization details, see the Supporting Information).[31] They were designated OL-L, OL-M, and OL-H according to the PLA volume fraction (f_{PLA}) of 6, 13, and 20%, respectively (Figure S1 and Table S1). They all form micelles in water (Figure S2). In a typical adhesive formulation, a 50 wt % aqueous solution of OL is mixed with a 50 wt % TA solution. The TA solution volume is adjusted to be 5 mol % TA relative to the PEO repeating units. Coacervates with a bright brown color phase separate out of the solution and sink to the bottom of the vessel (Figure 1f). A ^{1}H NMR spectrum of OL-M in deuterated water shows signals corresponding to PEO protons only, consistent with the formation of micelles with a PEO corona and a PLA core (Figure S3). The addition of TA fully suppresses the PEO signal, indicating a strong TA–PEO association. A shift in the C–O–C stretching vibrational band to a lower wavenumber supports hydrogen bonding of the TA hydroxyl groups with the ethereal oxygens in the PEO (Figure S4).

We probed the viscoelastic behavior of OLs and their mixtures with TA (OL/TAs) by dynamic shear measurements, compared to PEO as a reference (Figure 2). At room temperature, 50 wt % aqueous solutions of PEO and OL-L were liquid, showing very low storage moduli (G'), smaller than 10 Pa, and could not be accurately measured (Figure S5). The OL-M and OL-H solutions formed gels and did not flow. A plateau in G' was observed, which was higher than the loss moduli (G'') over the entire investigated range of angular frequency (ω), indicating that a network structure forms by packing of the OL micelles, imparting the elastic response.

https://doi.org/10.1021/jacsau.2c00241
JACS Au XXXX, XXX, XXX–XXX

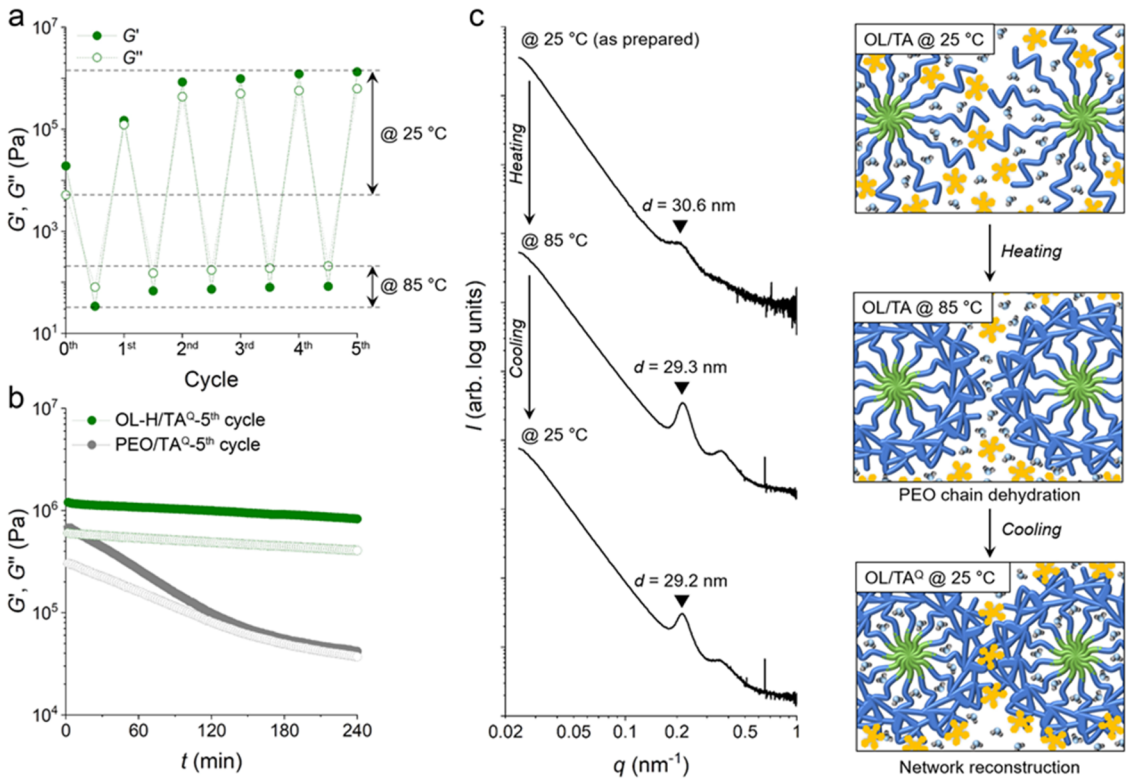

Figure 3. Heat-treated strengthening of OL/TA. (a) G' and G'' of OL-H/TA obtained at ω = 1 rad s^{-1} and γ = 0.1% over five heating−cooling cycles. In each cycle, the temperature was increased to 85 °C at a rate of 20 °C min^{-1} and maintained for 5 min. Then, the sample was cooled back to 25 °C and rested for 5 min. (b) Relaxation of OL-H/TA^Q and PEO/TA^Q over time probed by the change in G' (filled circle) and G'' (open circle) at ω = 1 rad s^{-1} and γ = 0.1%. (c) One-dimensional small-angle X-ray scattering (SAXS) profiles of OL-H/TA upon heating to 85 °C and cooling back to 25 °C. The proposed structural transition including dehydration upon heating and redistribution of the hydrogen bonds during cooling is schematically illustrated along the SAXS data.

TA increases the viscosity of the solution upon addition. A power law dependence of $G'' \sim \omega$ is apparent in the PEO/TA and OL-L/TA, while G' does not follow the ω^2 scaling typically observed in a viscous fluid (Figure 2a,b). The slope of G' and G'' becomes near 0.5 in the high-frequency regime. This is consistent with the sticky Rouse model that describes associative polymer networks, in this case, mediated by hydrogen bonding of the PEO with TA.[32,33]

OL-M/TA and OL-H/TA behaved as a viscoelastic solid with an increase in G' and G'' with increasing frequency (Figure 2c,d). G' also increased with the PLA content, indicating that the PLA micellar core is isolated from the PEO−TA network swollen in water. A 900 times higher G' was observed in OL-H/TA compared to PEO/TA (Figure 2e). The stability of the network was also enhanced by increasing the PLA fraction, as evidenced by the crossover between G' and G'' appearing at a higher strain in the amplitude sweep (Figure S6).

We also investigated the effect of the amount of TA on the rheological properties of OL-M/TA (Figures 2f and S7). Adding more TA increased G'' more strongly than G' and collapsed the gel at a smaller strain, suggesting that the PEO−TA network dominates the response at high TA loading. G' showed a maximal value at a 5 mol % TA loading relative to PEO repeating units ([EO]/[TA] = 20:1). This value coincides with the previously reported optimal PEO:TA ratio, which showed the strongest adhesion.[16] Above this ratio, the increased number of unbound TA molecules may result in a decrease in G' (Figure S7).

Heat-Treated Strengthening

The strength of the OL/TA hydrogels was remarkably enhanced by heating−cooling cycles. Figure 3a shows the change in moduli of the OL-H/TA upon heating to 85 °C and cooling back to 25 °C (for the whole frequency sweep data, see Figure S8). At 85 °C, some water squeezes out of the hydrogel and the phase-separated material behaves as a liquid with a G' of 30 Pa. Upon cooling to room temperature, the gel state is quickly restored and the released water is adsorbed back. Strikingly, G' and G'' increased about 10-fold compared to the as-produced gel without heating. Mechanical properties were further enhanced by repeating the successive temperature cycles up to five times, resulting in 100 times higher G', on the order of 1 MPa. Simply cooling the heated gel in the air also gives the hardened material, which is denoted OL-H/TA^Q. This heat-treating process is conceptually reminiscent of steel hardening by thermal quenching.[34]

The heat-treated strengthening was also observed for OL-M/TA and even PEO/TA, indicating that the phenomenon is related to the PEO−TA interaction (Figures S9 and S10). The change was the most dramatic in PEO/TA, probably because of the higher PEO fraction, and turned the material into a gel state with a G' of >1 MPa. However, the improvements only lasted temporarily in PEO/TA^Q: the material quickly lost the moduli and went back to liquid after approximately 2 h at room temperature (Figure 3b). In contrast, the OL-H/TA^Q successfully sustained the increased moduli in the gel state over a prolonged time. After 10 h, G' was still higher than 0.4 MPa.

https://doi.org/10.1021/jacsau.2c00241
JACS Au XXXX, XXX, XXX−XXX

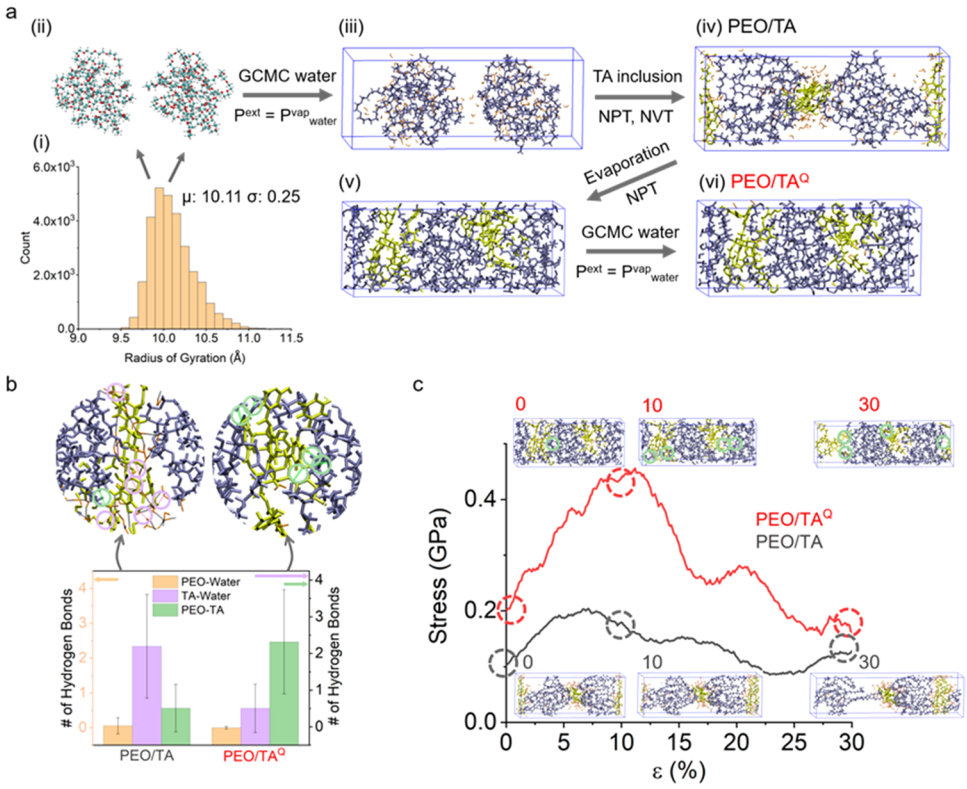

Figure 4. MD simulations of PEO−TA interfaces. (a) Simulation procedure to model the PEO−TA interface. PEO/TA and PEO/TA^{Q} mimic the structures before and after the temperature cycle, respectively. PEO: blue, water: orange, and TA: yellow. (b) Magnified views of interfacial structures (upper panels) showing hydrogen bonds by dashed lines, and the average number of hydrogen bonds between PEO−water, TA−water, and PEO−TA (lower panel). (c) MD-simulated stress−strain curve of PEO/TA and PEO/TA^{Q} under the *z*-direction axial elongation. The structures at 0, 10, and 30% of strain are represented in insets.

We believe that the heat-treated strengthening originates from the temperature-dependent solubility of PEO in water. With increasing temperature, the PEO chains are known to be relatively dehydrated and become less soluble in aqueous environments.[35] A gel-to-sol transition is known to occur in aqueous solutions of OL and related amphiphilic block copolymers as a function of the polymer concentration and composition.[36] This is ascribed to an upper critical solution temperature, which causes a breakdown in the micellar packing network by increased chain mobility and reduced micellar volume. The temperature-dependent frequency sweep data of both OL-M and OL-M/TA were consistent with a gel-to-sol transition above 75 °C (Figure S11). The hydrogen bonding mediated by TA does not seem to largely alter the transition temperature. We note this temperature is also above the glass transition temperature of PLA (~52 °C).[37]

We probed changes in the micellar morphology upon heating−cooling by synchrotron small-angle X-ray scattering (SAXS) (Figures 3c and S12−S15). Distinct scattering features were discernable in the OL aqueous solutions at room temperature, which were consistent with disordered micellar packing in general (Figure S12). The addition of TA suppresses scattering intensities considerably and can be attributed to the increased heterogeneity in the micellar packing and also the decreased electronic density contrast of the PLA core to the PEO/TA/water surrounding. Nonetheless, a broad principal scattering peak could be discerned in the SAXS profile of the as-prepared OL-H/TA responsible for micelle−micelle correlations, with an average intermicellar spacing (*d*) of 31 nm (Figure 3c).

The micellar network swells slightly, by 6%, in the presence of TA. Heating to 85 °C refined the scattering patterns of both the OL-H and OL-H/TA, accompanied by higher-order scattering functions (Figure S13). A strong increase in the scattering intensity was particularly noticed from OL-H/TA. Improved lateral ordering and a narrower interface in the micellar morphology are indicative of the facilitated exchange of OL chains with increased mobility in the sol state, even when TA is present (Figure S14). The slightly decreased spacing is also consistent with a reduction in the micellar volume by the partial collapse of the PEO corona (Figure S15). Interestingly, the refined scattering features in OL-H/TA persist upon cooling to room temperature, with a negligible change in *d*. The temperature-dependent changes were not obvious in the SAXS data of the other OL/TAs with lower PLA fractions because of weak scattering intensities (Figure S13).

The temporary mechanical enhancement of PEO/TA after the temperature cycle suggests that PEO prefers to associate with TA during rehydration, and this increases the effective density of the hydrogen bonds. The resulting transient network would relax quickly at room temperature by the hydration-driven redistribution of TA and the PEO chains. Since the glassy PLA core hinders the rearrangement of PEO chains at room temperature in OL/TA, the PEO−TA matrix is thought to retain the densified hydrogen bonding clusters with a much longer relaxation time. Together with the improved long-range order, the micellar packing network with the increased cross-linking density boosts both the elastic and viscous responses. The mechanical responses would be further amplified until the

https://doi.org/10.1021/jacsau.2c00241
JACS Au XXXX, XXX, XXX−XXX

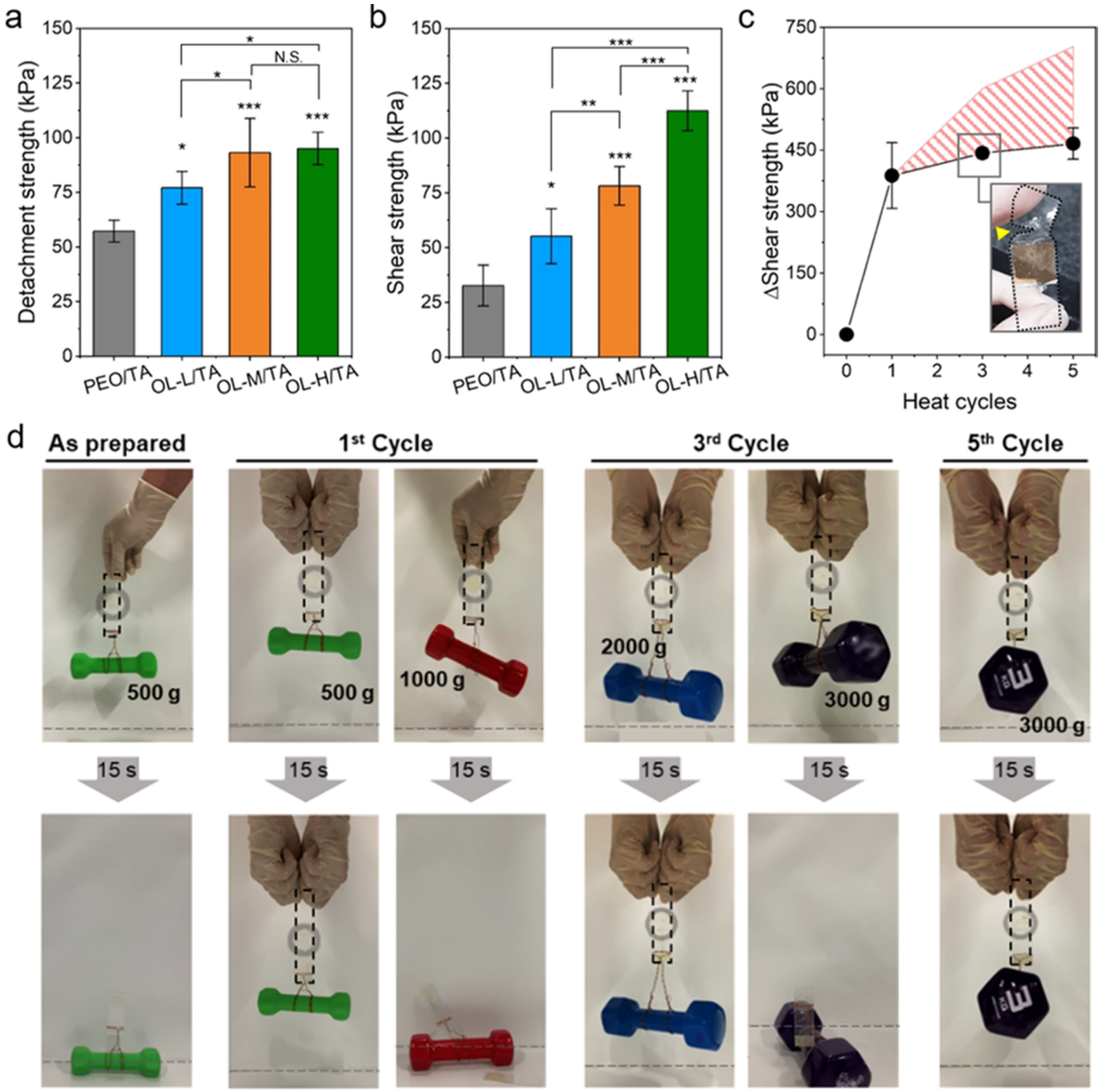

Figure 5. Adhesive performances of OL/TAs. (a, b) Detachment strength (a) and shear strength (b) of OL/TAs (n = 5). PET was used as a substrate. A significant difference is indicated by *P < 0.05 and ***P < 0.0005 in OL/TAs versus PEO/TA and *P < 0.05, **P < 0.005, and ***P < 0.0005 between OL-L/TA, OL-M/TA, and OL-H/TA. N.S. indicates not significant. (c) Dependence of the heating−cooling cycles on shear strength of OL-M/TA on PET films (n = 5). Black circles indicate experimentally determined data points. The inset photo shows the substrate failure of a specimen after three heat cycles of the specimen (indicated by the yellow arrowhead). Pink circles represent predicted values based on the modulus trend assuming the absence of substrate failure. (d) Photos showing dumbbells being lifted using the glass substrates bonded with OL-M/TA after an increasing number of heat cycles (see Video S1). The bonding time was 20 min at RT. Photos were taken after 15 s of lifting. The glass substrates are marked by black dashed rectangles. Gray circles and red arrowheads indicate undetached and detached adhesion areas, respectively.

PEO−TA interaction efficiency is maximized during the repeated dehydration−rehydration process of the PEO corona over the temperature cycles.

We performed molecular dynamics (MD) simulations,[38−47] as outlined in Figure 4a, to understand the origin of redistribution of hydrogen bonds during the temperature cycle. The random coil structures of PEO were sampled using the scaled effective solvent method,[45] and two characteristic conformers were obtained and then included in the three-dimensional (3D) periodic simulation cell. The PEO chains were hydrated using the grand canonical Monte Carlo (GCMC) simulation by setting the external pressure to be water vapor pressure at room temperature (Figure S16). TA molecules were sandwiched in between the PEO chains and the entire system was equilibrated at 300 K. The obtained structure was considered to model the PEO−TA interface before heating.

To mimic dehydration upon heating, we randomly evaporated water molecules to completely dehydrate the system during MD simulation. We then rehydrated the system using GCMC to model the PEO−TA interface in PEO/TA^{Q} (Figure S17). The number of hydrogen bonds between PEO with TA increased fourfold in PEO/TA^{Q} compared to PEO/TA (Figure 4b). Prior to dehydration, both PEO and TA reside in their own hydration shells and form a relatively small number of PEO−TA hydrogen bonds. The removal of water facilitates hydrogen bonding of PEO with TA. Replacing PEO with water as a hydrogen bonding partner for TA seems less favored during rehydration in the densified structure, causing impeded reinclusion of water. We further computationally

https://doi.org/10.1021/jacsau.2c00241
JACS Au XXXX, XXX, XXX−XXX

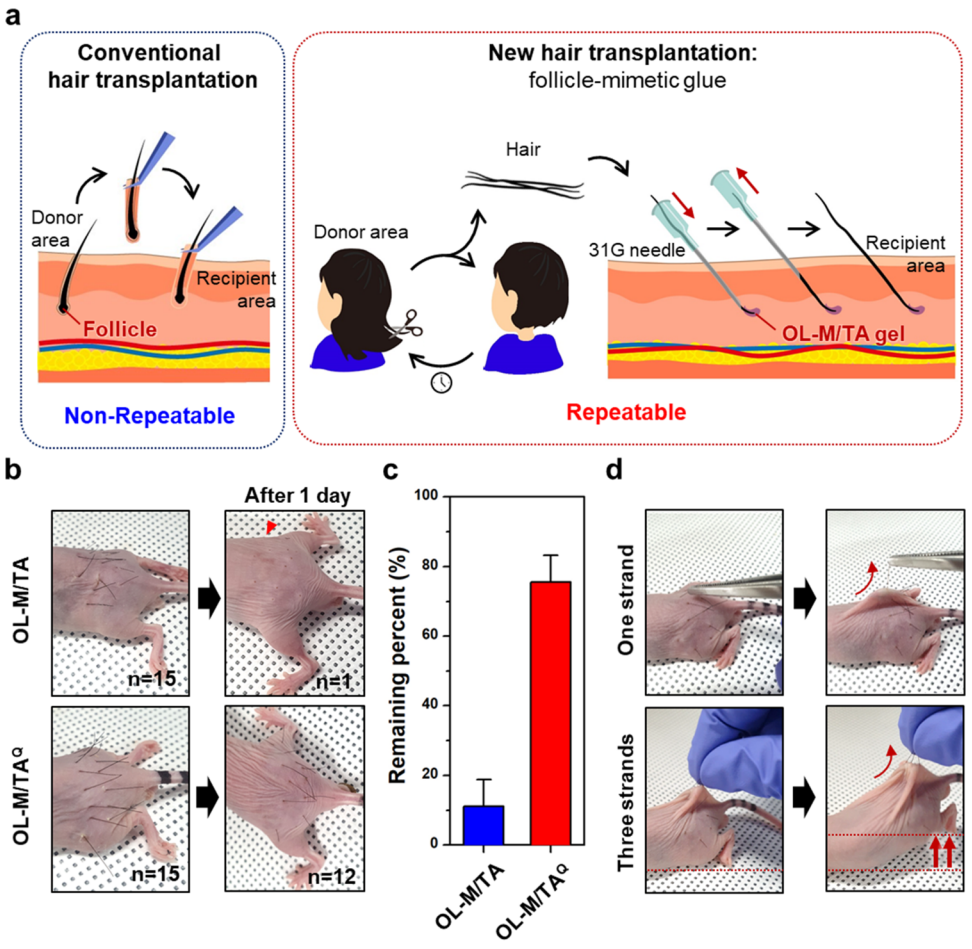

Figure 6. Application of OL/TA glue for hair transplantation surgery. (a) Schematic illustrations of the conventional hair transplantation procedure (left box) and the new hair transplantation approach using OL/TA as follicle-mimetic glue (right box). (b) Photographs of the remaining hair strands 1 day after hair transplantation using as-prepared OL-M/TA (top) and heat-treated OL-M/TA^{Q} (bottom). A red arrowhead indicates the remaining single strand in the OL-M/TA case. (c) Percentage of remaining hair strands 1 day postoperation using OL-M/TA (blue) and OL-M/TA^{Q} (red). The error bar indicates standard deviations (n = 3). (d) Photographs showing the adhesiveness of OL-M/TA^{Q} by pulling the transplanted hair strands 1 day after hair transplantation.

investigated the mechanical properties of two models by calculating stress−strain curves (Figure 4c). Young's modulus of PEO/TA^{Q} was found to be 1.5 times larger than that of PEO/TA, which is ascribed to the densified interfacial hydrogen bonds and consistent with the experimentally observed boost in the mechanical properties.

Adhesion Performances

As expected from the viscoelastic properties, OL/TAs exhibited superior adhesion performance compared with PEO/TA lacking the PLA block (Figure 5). Detachment (tensile) strength of two poly(ethylene terephthalate) (PET) films bonded using OL/TAs was measured (for the test configurations, see Scheme S1). Compared to 57.2 ± 5.0 kPa with PEO/TA, the detachment strength increased with increasing the PLA fraction up to 95.1 ± 7.4 kPa in OL-H/TA (Figure 5a). We observed the same trend in T-peeling tests (Figure S18). The peeling force increased up to 30 N m^{-1} for OL-H/TA.

Consistent with the G' increase, this is indicative of the higher cohesive strength attained by the micellar packing network.[48] Shear strength showed a similar trend with even a larger increase: >100 kPa was achieved with OL-H/TA, which is more than a threefold increase compared to PEO/TA (Figure 5b). In spite of the high cohesion strength, OL-M/TA and OL-H/TA retained good tackiness provided by the wet PEO−TA matrix.

We further examined the shear strength of OL-M/TA^{Q} as a function of the temperature cycle number by heating and cooling the bonded PET substrates (Figure 5c). Consistent with the enhancement in G' and G'', a large increase in the shear strength of ∼400 kPa was observed after the first cycle followed by further augmentation over the four successive cycles. Interestingly, the PET substrate itself was fractured after the third cycle, that is, OL-M/TA^{Q} glue can withstand much higher shear strength than the measured values.

Dumbbell lifting with OL-M/TA^{Q}-bonded glass substrates indeed demonstrated further improved adhesion performance (Figure 5d and Video S1). The strong adhesion of OL/TA is surprising, given that the adhesion strength between the adhesive with the substrate is correlated to a higher G'' and typically decreases with increasing cohesive strength.[48] The tradeoff relationship seems to be compromised to some extent in the OL/TA system as both G' and G'' increase with increasing PLA content and also over the temperature cycles. Heating to high temperature close to the gel-to-sol transition also increases fluidity (characterized by higher tan $\delta = G''/G'$) and ensures good contact to the substrate surface.[49] We note

https://doi.org/10.1021/jacsau.2c00241
JACS Au XXXX, XXX, XXX−XXX

that such dynamic material properties are one of the key characteristics of self-assembled materials that can be modulated in response to external stimuli. We also noted that the water loss during the temperature cycles was minimal (Figure S19).

Follicle-Free Hair Transplantation

We established a suitable in vivo model to utilize the unique properties of the heat-treated adhesion reinforcement of OL/TA gel: hair transplantation (Figure 6). A conventional hair transplantation involves a collection of follicles from patients' tissue such as the back scalp, followed by insertion into a recipient area (Figure 6a, left section). Typically, a large piece of the scalp is resected and closed by pulling the surrounding skin. This surgery is nonrepetitive (two times at most) due to the limited donor skin area. Implanting more hair is not possible although hair loss in the implanted area has been commonly reported.

Here, we introduce a new concept called follicle-free hair transplantation (Figure 6a, right section) to overcome the aforementioned limitations. This follicle-free transplantation uses tissue adhesives applied at the follicle side end of each hair. We hypothesized that the glue could fix hair strands by connecting between the hair surface and the subcutaneous tissue in the recipient area, just like a hair follicle. The surgery does not require invasive tissue resections and no follicle extraction procedures are needed. It is repetitive due to the continuous supply of hair strands from the donor's haircut, and direct transplantation of the desired length or color of hair should be also possible. With these possible outcomes in mind, we demonstrate fixing hair strands as a proof of concept.

We transplanted 15 strands of human hair onto the dorsal skin of nude mice (n = 3) using OL-M/TA as a model adhesive (Figures 6b,c and S20). OL-M/TA^{Q} glue was prepared by heating up to 75 °C to make it into a sol and it was applied to the end of a hair strand. We lowered the heating temperature to 75 °C to avoid thermal damage to the tissue: the final temperature of the glue was 40−50 °C at the moment of injection. Most of the hair strands (76%) remained when OL-M/TA^{Q} was used, while only a few strands of the unheated OL-M/TA glue remained (11%). This clearly shows the advantages of the OL/TA^{Q} glue. Its fluidity can be increased by heating to ease tissue penetration and strengthen adhesion at room temperature. Implanting bare hair strands without applying the glue left no hair strands (Figure S21).

When a single hair strand transplanted with the OL/TA^{Q} glue was pulled using forceps, the strand showed stable adhesion, enough to raise the tissue (Figure 6c). Even the whole mouse body was lifted when pulling with three hair strands, convincingly demonstrating strong adhesion to tissue and thereby the excellent potential for hair transplantation. We also note that the OL/TA gel exhibited minimal irritation to the skin even when it was injected, supporting the compatibility of the OL/TA as a tissue adhesive (Figure S22). The OL/TA gel was also degraded within 14 days when it was injected subcutaneously into hairless mice (Figure S23).

CONCLUSIONS

We developed a strong, biocompatible, and biodegradable waterborne glue by combining a block copolymer self-assembly with noncovalent interactions. Our modular design combines all biocompatible components, an amphiphilic diblock copolymer PEO-*b*-PLA, and TA as a natural polyphenol capable of multiple hydrogen bonds. The block copolymer micelles formed in water were bridged with TA to produce a viscoelastic solid. While the sticky features of the hydrogen-bonded network mediated by TA were retained, the hydrophobic PLA micellar core reinforced the material, boosting cohesive strength.

Utilizing the temperature-dependent hydration behavior of the PEO corona, the material was self-strengthened by iteratively applying heating−cooling cycles. The adhesive became more fluidic as it approached the gel-to-sol transition during heating, and further hardened upon cooling by the more effective association in the network structure.

Noninvasive, sustainable, follicle-free hair transplantation was demonstrated with the heat-treated adhesive. Given the wide range of material properties introduced in this study, the diverse synthetic freedom of block copolymer systems, and the versatile self-assembling morphologies accessible by block copolymers, this study opens a new route to designing biomedical adhesives with dynamic, tunable, yet improved performances for target applications.

METHODS

Materials

Unless mentioned otherwise, the chemicals were used as purchased. 1,8-Diaza-bicyclo[5.4.0]undec-7-ene (DBU), tannic acid, and methoxy-terminated poly(ethylene oxide) (PEO-OH, number average molar mass = 20 kg mol^{-1}) were purchased from Sigma-Aldrich (St. Louis, MO). D,L-Lactide (LA) was kindly provided by Corbion Purac (Amsterdam, Netherlands) and stored in a glovebox after recrystallization from ethyl acetate. Benzoic acid was purchased from Daejung chemicals (Siheung, Korea). HPLC-grade dichloromethane (DCM) was purchased from Burdick & Jackson (Morristown, NJ) and purified using a solvent purification system (C&T International, Suwon, Korea).

Synthesis of PEO-*b*-PLA

The synthesis of OL-H is given as an example. A polymerization mixture containing PEO-OH (2.000 g, 0.1000 mmol) and D,L-lactide (0.721 g, 10.0 mmol) in DCM (20 mL) was prepared in a glovebox. A stock solution of DBU in DCM (7.6 wt %, 0.1 mL, 0.072 mmol) was added to the reaction flask and stirred for 8 min at an ambient condition. Then, benzoic acid (8.4 mg, 1.4 μmol) was added to stop the polymerization. The product was purified by dialysis against methanol at an ambient condition for 24 h. The resulting polymer was collected by evaporation and dried under a vacuum at 40 °C overnight.

The identical protocol was used for the syntheses of OL-L and OL-M by varying the amount of D,L-lactide.

Preparation of OL/TA

OL-M/TA is given as an example. Aqueous solutions of OL-M and TA (50 wt %) were prepared by dissolving OL-M (0.1999 g) and TA (0.3319 g, 0.1951 mmol, 5 mol % to the PEO repeating units) in deionized water at 60 °C, respectively. The TA solution was added to the OL-M solution, mixed with a spatula, and then stirred overnight. The bright brown-colored mixture was settled down to the bottom using a centrifuge Combi R514R (Hanil Inc., Daejeon, Korea) with 5000 G for 15 min and separated from the supernatant.

PEO/TA and other OL/TA hydrogels were prepared by following the protocol described above.

Additional details for material characterization, computation, adhesion test, and animal experiments are presented in the Supporting Information.

https://doi.org/10.1021/jacsau.2c00241
JACS Au XXXX, XXX, XXX−XXX

■ ASSOCIATED CONTENT

Supporting Information

The Supporting Information is available free of charge at https://pubs.acs.org/doi/10.1021/jacsau.2c00241.

Additional methods and data for material characterization including ^{1}H NMR spectra, SEC traces, DLS, FTIR spectra, oscillatory shear and SAXS measurement, computational details, adhesion test, biodegradation test, intradermal reaction test, and in vivo hair transplantation (PDF)

Video showing dumbbells being lifted using the glass substrates bonded with OL-M/TA after an increasing number of heat cycles (Video S1) (MPG)

■ AUTHOR INFORMATION

Corresponding Authors

Haeshin Lee − *Department of Chemistry, Korea Advanced Institute of Science and Technology (KAIST), Daejeon 34141, Korea;* orcid.org/0000-0003-3961-9727; Email: estoeric93@kaist.ac.kr

Myungeun Seo − *Department of Chemistry, Korea Advanced Institute of Science and Technology (KAIST), Daejeon 34141, Korea; KAIST Institute for Nanocentury, KAIST, Daejeon 34141, Korea;* orcid.org/0000-0002-5218-3502; Email: seomyungeun@kaist.ac.kr

Authors

Jongmin Park − *Department of Chemistry, Korea Advanced Institute of Science and Technology (KAIST), Daejeon 34141, Korea;* Present Address: Advanced Functional Polymers Research Center, Korea Research Institute of Chemical Technology (KRICT), Daejeon 34114, Korea

Eunsook Park − *Department of Chemistry, Korea Advanced Institute of Science and Technology (KAIST), Daejeon 34141, Korea*

Siyoung Q. Choi − *Department of Chemical and Biomolecular Engineering, KAIST, Daejeon 34141, Korea;* orcid.org/0000-0002-6020-3091

Jingxian Wu − *Department of Chemistry, Korea Advanced Institute of Science and Technology (KAIST), Daejeon 34141, Korea*

Jihye Park − *Department of Chemistry, Korea Advanced Institute of Science and Technology (KAIST), Daejeon 34141, Korea;* orcid.org/0000-0002-4704-5201

Hyeonju Lee − *Department of Chemistry, Korea Advanced Institute of Science and Technology (KAIST), Daejeon 34141, Korea*

Hyungjun Kim − *Department of Chemistry, Korea Advanced Institute of Science and Technology (KAIST), Daejeon 34141, Korea;* orcid.org/0000-0001-8261-9381

Complete contact information is available at: https://pubs.acs.org/10.1021/jacsau.2c00241

Author Contributions

$^{\perp}$J.P. and E.P. contributed equally to this work. M.S. conceptualized the idea. J.P. performed material synthesis, characterization, and oscillatory shear and SAXS measurement. E.P. performed an adhesion test and an intradermal reaction test. J.P., H.L., and H.K. performed computational analysis. M.S. and J.P. wrote the original draft. Every author reviewed and edited the manuscript. M.S. and H.L. supervised all aspects of the research. CRediT: **Jongmin Park** investigation, methodology, visualization, writing-original draft, writing-review & editing; **Eunsook Park** investigation, methodology, visualization, writing-review & editing; **Siyoung Q. Choi** methodology, writing-review & editing; **jingxian wu** investigation, methodology, visualization, writing-review & editing; **Jihye Park** investigation, methodology, visualization, writing-review & editing; **Hyeonju Lee** investigation, methodology, visualization, writing-review & editing; **Hyungjun Kim** methodology, writing-review & editing; **Haeshin Lee** funding acquisition, methodology, supervision, writing-review & editing; **Myungeun Seo** conceptualization, funding acquisition, methodology, project administration, supervision, writing-original draft, writing-review & editing.

Funding

This research was supported by the Basic Science Research Program through the National Research Foundation of Korea (NRF) funded by the Ministry of Education (2019R1I1A2A01063804) and the Center for Multiscale Chiral Architectures funded by the Ministry of Science and ICT of Korea (2018R1A5A1025208), the Bio-Industrial Technology Development Program funded by the Ministry of Trade, Industry and Energy (20008628), and the KRICT Core Project (SS2121-20). Experiments at the Pohang Accelerator Laboratory (PAL) were supported in part by the Ministry of Science and ICT and POSTECH.

Notes

The authors declare the following competing financial interest(s): The authors are declared to be inventors on a patent filed by the Korea Advanced Institute of Science and Technology related to the work presented here.
The authors are declared to be inventors on a patent filed by the Korea Advanced Institute of Science and Technology related to the work presented here.

■ REFERENCES

(1) Pinnaratip, R.; Bhuiyan, M. S. A.; Meyers, K.; Rajachar, R. M.; Lee, B. P. Multifunctional biomedical adhesives. *Adv. Healthcare Mater.* **2019**, *8*, No. 1801568.

(2) Bhagat, V.; Becker, M. L. Degradable adhesives for surgery and tissue engineering. *Biomacromolecules* **2017**, *18*, 3009−3039.

(3) Leggat, P. A.; Smith, D. R.; Kedjarune, U. Surgical applications of cyanoacrylate adhesives: a review of toxicity. *ANZ J. Surg.* **2007**, *77*, 209−213.

(4) Ryu, J. H.; Kim, H. J.; Kim, K.; Yoon, G. S.; Wang, Y.; Choi, G.-S.; Lee, H.; Park, J. S. Multipurpose intraperitoneal adhesive patches. *Adv. Funct. Mater.* **2019**, *29*, No. 1900495.

(5) Kim, K.; Ryu, J. H.; Koh, Mi.-Y.; Yun, S. P.; Kim, S.; Park, J. P.; Jung, C.-W.; Lee, M. S.; Seo, H.-I.; Kim, J. H.; Lee, H. Coagulopathy-independent, bioinspired hemostatic materials: A full research story from preclinical models to a human clinical trial. *Sci. Adv.* **2021**, *7*, No. eabc9992.

(6) Lee, C.; Shin, J.; Lee, J. S.; Byun, E.; Ryu, J. H.; Um, S. H.; Kim, D.-I.; Lee, H.; Cho, S.-W. Bioinspired, calcium-free alginate hydrogels with tunable physical and mechanical properties and improved biocompatibility. *Biomacromolecules* **2013**, *14*, 2004−2013.

(7) Hong, S. H.; Shin, M.; Lee, J.; Ryu, J. H.; Lee, S.; Yang, J. W.; Kim, W. D.; Lee, H. STAPLE: Stable alginate gel prepared by linkage exchange from ionic to covalent bonds. *Adv. Healthcare Mater.* **2016**, *5*, 75−79.

(8) Park, E.; Lee, J.; Huh, K. M.; Lee, S. H.; Lee, H. Toxicity-attenuated glycol chitosan adhesive inspired by mussel adhesion mechanisms. *Adv. Healthcare Mater.* **2019**, *8*, 1900275−1900282.

(9) Park, J. Y.; Yeom, J.; Kim, J. S.; Lee, M.; Lee, H.; Nam, Y. S. Cell-repellant dextran coatings of porous titania using mussel adhesion chemistry. *Macromol. Biosci.* **2013**, *13*, 1511−1519.
(10) Lee, H.; Lee, K. D.; Pyo, K. B.; Park, S. Y.; Lee, H. Catechol-grafted poly(ethylene glycol) for PEGylation on versatile substrates. *Langmuir* **2010**, *26*, 3790−3793.
(11) Zhan, K.; Kim, C.; Sung, K.; Ejima, H.; Yoshie, N. Tunicate-inspired gallol polymers for underwater adhesive: a comparative study of catechol and gallol. *Biomacromolecules* **2017**, *18*, 2959−2966.
(12) Kim, M.; Ondrusek, B. A.; Lee, C.; Douglass, W. G.; Chung, H. Synthesis of lightly crosslinked zwitterionic polymer-based bioinspired adhesives for intestinal tissue sealing. *J. Polym. Sci., Part A: Polym. Chem.* **2018**, *56*, 1564−1573.
(13) Kim, M.; Chung, H. Photo-responsive bio-inspired adhesives: facile control of adhesion strength via a photocleavable crosslinker. *Polym. Chem.* **2017**, *8*, 6300−6308.
(14) Pramudya, I.; Kim, C.; Chung, H. Synthesis and adhesion control of glucose-based bioadhesive via strain-promoted azide−alkyne cycloaddition. *Polym. Chem.* **2018**, *9*, 3638−3650.
(15) Kim, M.; Butler, M. F.; Pramudya, I.; Lee, C.; Kim, S.; Chung, H. Metal-free electrically conductive bioinspired adhesive polymers. *Chem. Mater.* **2019**, *31*, 8358−8365.
(16) Kim, K.; Shin, M.; Koh, M.-Y.; Ryu, J. H.; Lee, M. S.; Hong, S.; Lee, H. TAPE: a medical adhesive inspired by a ubiquitous compound in plants. *Adv. Funct. Mater.* **2015**, *25*, 2402−2410.
(17) Fan, H.; Wang, J.; Zhang, Q.; Jin, Z. Tannic acid-based multifunctional hydrogels with facile adjustable adhesion and cohesion contributed by polyphenol supramolecular chemistry. *ACS Omega* **2017**, *2*, 6668−6676.
(18) Sun, Y.; Liu, Z.; Chen, F.; Xu, M.; Zhang, J.; Li, W. Hierarchical cross-linked poly(caprolactone-co-urethane) toward connective tissue-like properties and multifunctional integration. *Chem. Mater.* **2019**, *31*, 9295−9306.
(19) Nam, H. G.; Nam, M. G.; Yoo, P. J.; Kim, J.-H. Hydrogen bonding-based strongly adhesive coacervate hydrogels synthesized using poly(N-vinylpyrrolidone) and tannic acid. *Soft Matter* **2019**, *15*, 785−791.
(20) Dang, Q. D.; Moon, J. R.; Jeon, Y. S.; Kim, J.-H. Supramolecular adhesive gels based on biocompatible poly(2-ethyl-2-oxazoline) and tannic acid via hydrogen bonding complexation. *J. Appl. Polym. Sci.* **2020**, *137*, 48285−48292.
(21) Lee, D.; Hwang, H.; Kim, J.-S.; Park, J.; Youn, D.; Kim, D.; Hahn, J.; Seo, M.; Lee, H. VATA: a poly(vinyl alcohol)- and tannic acid-based nontoxic underwater adhesive. *ACS Appl. Mater. Interfaces* **2020**, *12*, 20933−20941.
(22) Li, B.; Whalen, J. J., III; Humayun, M. S.; Thompson, M. E. Reversible bioadhesives using tannic acid primed thermally-responsive polymers. *Adv. Funct. Mater.* **2020**, *30*, No. 1907478.
(23) Quideau, S.; Deffieux, D.; Douat-Casassus, C.; Pouységu, L. Plant polyphenols: chemical properties, biological activities, and synthesis. *Angew. Chem., Int. Ed.* **2011**, *50*, 586−621.
(24) Guo, J.; Suma, T.; Richardson, J. J.; Ejima, H. Modular assembly of biomaterials using polyphenols as building blocks. *ACS Biomater. Sci. Eng.* **2019**, *5*, 5578−5596.
(25) Cohn, D.; Younes, H. Biodegradable PEO/PLA block copolymers. *J. Biomed. Mater. Res.* **1988**, *22*, 993−1009.
(26) Conn, D.; Younes, H. Compositional and structural analysis of PELA biodegradable block copolymers degrading under in vitro conditions. *Biomaterials* **1989**, *10*, 466−474.
(27) Conn, R. E.; Kolstad, J. J.; Borzelleca, J. F.; Dixler, D. S.; Filer, L. J., Jr; LaDu, B. N., Jr; Pariza, M. W. Safty assessment of polylactide (PLA) for use as a food-contact polymer. *Food Chem. Toxicol.* **1995**, *33*, 273−283.
(28) Jeong, B.; Bae, Y. H.; Lee, D. S.; Kim, S. W. Biodegradable block copolymers as injectable drug-delivery systems. *Nature* **1997**, *388*, 860−862.
(29) Cho, H.; Gao, J.; Kwon, G. S. PEG-b-PLA micelles and PLGA-b-PEG-b-PLGA sol−gels for drug delivery. *J. Controlled Release* **2016**, *240*, 191−201.
(30) Repp, L.; Rasoulianboroujeni, M.; Lee, H. J.; Kwon, G. S. Acyl and oligo(lactic acid) prodrugs for PEG-b-PLA and PEG-b-PCL nano-assemblies for injection. *J. Controlled Release* **2021**, *330*, 1004−1015.
(31) Sherck, N. J.; Kim, H. C.; Won, Y.-Y. Elucidating a unified mechanistic scheme for the DBU-catalyzed ring-opening polymerization of lactide to poly(lactic acid). *Macromolecules* **2016**, *49*, 4699−4713.
(32) Rubinstein, M.; Semenov, A. N. Thermoreversible gelation in solutions of associating polymers. 2. Linear dynamics. *Macromolecules* **1998**, *31*, 1386−1397.
(33) Golkaram, M.; Loos, K. A critical approach to polymer dynamics in supramolecular polymers. *Macromolecules* **2019**, *52*, 9427−9444.
(34) MacKenzie, D. S. History of quenching. *Int. Heat Treat. Surf. Eng.* **2008**, *2*, 68−73.
(35) Shikata, T.; Okuzono, M.; Sugimoto, N. Temperature-dependent hydration/dehydration behavior of poly(ethylene oxide)s in aqueous solution. *Macromolecules* **2013**, *46*, 1956−1961.
(36) Choi, S. W.; Choi, S. Y.; Jeong, B.; Kim, S. W.; Lee, D. S. Thermoreversible gelation of poly(ethylene oxide) biodegradable polyester block copolymers. II. *J. Polym. Sci., Part A: Polym. Chem.* **1999**, *37*, 2207−2218.
(37) Andrews, R. J.; Grulke, E. A. Glass Transition Temperature of Polymers. In *Polymer Handbook*, 4th ed.; Brandrup, J.; Immergut, E. H.; Grulke, E. A., Eds.; John Wiley & Sons, Inc.: New York, 1998; pp VI/193−VI/253.
(38) Thompson, A. P.; Aktulga, H. M.; Berger, R.; Bolintineanu, D. S.; Brown, W. M.; Crozier, P. S.; in't Veld, P. J.; Kohlmeyer, A.; Moore, S. G.; Nguyen, T. D.; Shan, R.; Stevens, M.; Tranchida, J.; Trott, C.; Plimpton, S. J. LAMMPS—a flexible simulation tool for particle-based materials modeling at the atomic, meso, and continuum scales. *Comput. Phys. Commun.* **2021**, *271*, No. 108171.
(39) Evans, D. J.; Holian, B. L. The Nose−Hoover thermostat. *J. Chem. Phys.* **1985**, *83*, 4069−4074.
(40) Parrinello, M.; Rahman, A. Polymorphic transitions in single crystals: a new molecular dynamics method. *J. Appl. Phys.* **1981**, *52*, 7182−7190.
(41) Becke, A. D. Density-functional thermochemistry. I. The effect of the exchange-only gradient correction. *J. Chem. Phys.* **1992**, *96*, 2155−2160.
(42) Grimme, S.; Antony, J.; Ehrlich, S.; Krieg, H. A consistent and accurate ab initio parametrization of density functional dispersion correction (DFT-D) for the 94 elements H-Pu. *J. Chem. Phys.* **2010**, *132*, No. 154104.
(43) Frisch, M. J.; Pople, J. A.; Binkley, J. S. Self-consistent molecular orbital methods 25. supplementary functions for gaussian basis sets. *J. Chem. Phys.* **1984**, *80*, 3265−3269.
(44) Bochevarov, A. D.; Harder, E.; Hughes, T. F.; Greenwood, J. R.; Braden, D. A.; Philipp, D. M.; Rinaldo, D.; Halls, M. D.; Zhang, J.; Friesner, R. A. Jaguar: a high-performance quantum chemistry software program with strengths in life and materials sciences. *Int. J. Quantum Chem.* **2013**, *113*, 2110−2142.
(45) Shin, H.; Pascal, T. A.; Goddard, W. A.; Kim, H. Scaled effective solvent method for predicting the equilibrium ensemble of structures with analysis of thermodynamic properties of amorphous polyethylene glycol-water mixtures. *J. Phys. Chem. B* **2013**, *117*, 916−927.
(46) Mayo, S. L.; Olafson, B. D.; Goddard, W. A. DREIDING: a generic force field for molecular simulations. *J. Phys. Chem. A* **1990**, *94*, 8897−8909.
(47) Jorgensen, W. L.; Chandrasekhar, J.; Madura, J. D.; Impey, R. W.; Klein, M. L. Comparison of simple potential functions for simulating liquid water. *J. Chem. Phys.* **1983**, *79*, 926−935.
(48) Chang, E. P. Viscoelastic windows of pressure-sensitive adhesives. *J. Adhesion* **1991**, *34*, 189−200.
(49) Moon, H.; Jeong, K.; Kwak, J.; Choi, S. Q.; Im, S. G. Solvent-free deposition of ultrathin copolymer films with tunable

https://doi.org/10.1021/jacsau.2c00241
JACS Au XXXX, XXX, XXX−XXX

viscoelasticity for application to pressure-sensitive adhesives. *ACS Appl. Mater. Interfaces* **2018**, *10*, 32668−32677.

Recommended by ACS

Interfacial Electrochemistry-Induced Detachable Adhesives with Ultra-High Bonding Strength and Detaching Efficiency

Min Wu, Yong Wei, *et al.*

AUGUST 30, 2022
ACS APPLIED MATERIALS & INTERFACES

READ

Hydrogen-Bonding Interaction-Driven Catechin Assembly into Solvent-Free Supramolecular Adhesive with Antidrying and Antifreezing Properties

Xiaoming Xie, Yulian Jiang, *et al.*

MAY 24, 2022
ACS APPLIED POLYMER MATERIALS

READ

Instant Strong and Responsive Underwater Adhesion Manifested by Bioinspired Supramolecular Polymeric Adhesives

Jiang Wu, Guangming Liu, *et al.*

MARCH 02, 2022
MACROMOLECULES

READ

Poly(propylene fumarate)-Based Adhesives with a Transformable Adhesion Force for Suture-Free Fixation of Soft Tissue Wounds

Xin Guan, Dagang Guo, *et al.*

MARCH 02, 2022
ACS APPLIED POLYMER MATERIALS

READ

Get More Suggestions >

https://doi.org/10.1021/jacsau.2c00241
JACS Au XXXX, XXX, XXX−XXX